PHYSICAL REVIEW A **84**, 021808(R) (2011)

Ab initio dissipative solitons in an all-photonic crystal resonator

Christoph Etrich,[1] Rumen Iliew,[1] Kestutis Staliunas,[2] Falk Lederer,[1] and Oleg A. Egorov[1]
[1]*Institute of Condensed Matter Theory and Solid State Optics, Friedrich-Schiller-Universität Jena, Max-Wien-Platz 1, D-07743 Jena, Germany*
[2]*Institució Catalana de Recerca i Estudis Avançats (ICREA), Departament de Física i Enginyeria Nuclear, Universitat Politècnica de Catalunya, Colom 11, E-08222 Terrassa, Barcelona, Spain*
(Received 11 April 2011; published 25 August 2011)

We identify dissipative solitons in a Kerr-nonlinear all-photonic crystal resonator by solving Maxwell's equations directly. The photonic crystal allows for diffraction management, leading to solitons with unique properties. These results are compared to a mean-field model based on Bloch waves, finding excellent agreement even for a high-contrast photonic crystal. By adjusting the quality factor and resonance frequencies of the resonator, optimal Bloch cavity solitons in terms of width and pump energy are identified. In particular, the width is independent of the quality factor, in contrast to the usual homogeneous cavity.

DOI: 10.1103/PhysRevA.84.021808 PACS number(s): 42.65.Tg, 42.60.Da, 42.65.Hw, 42.70.Qs

The existence of localized solutions or cavity solitons (CSs) in passive planar or ring resonators filled with a nonlinear material is an intriguing fact. Typically they are found in regions of bistability of the homogeneous solutions. Here they may be associated with a modulational instability of the upper branch. In the pioneering work [1] CSs are regarded as locked switching waves of stable homogeneous solutions. Bistability is not necessary to have CSs [2–4]. CSs belong to the class of dissipative solitons, because of the permanent energy exchange between the cavity and the environment.

Cavity solitons were found in resonators filled with different nonlinear materials. In Refs. [1] and [3] the Maxwell-Bloch equations for a two-level system were reduced to an equation for the field with a saturable Kerr nonlinearity. One- and two-dimensional (2D) stable CSs were found. In the simpler case of a Kerr medium, stable 2D CSs were identified in a narrow region in parameter space in Ref. [5]. In the case of the full Maxwell-Bloch equations for two levels, CSs were found in the limit of nascent bistability, where the dynamics can be described by the Swift-Hohenberg equation [6]. A more complicated case is a resonator filled with a material with a second-order nonlinearity. A variety of CSs was found. The system can be pumped either at the fundamental [4,7] or the second harmonic frequency (for an overview, see Ref. [8]).

An important example is a resonator filled with a semiconductor since it is more or less easily accessible to experiments. 2D CSs were predicted in Refs. [9] and [10] and found experimentally in Refs. [11] and [12]. Earlier experimental evidence of CSs was found in degenerate four-wave mixing [13].

Recently the idea of combining a nonlinear cavity with a photonic crystal (PhC) to tailor the diffraction properties of light was proposed [14,15]. For a weak modulation of the refractive index only in the transverse direction, one-dimensional CSs were found for third- or second-order nonlinearity [16,17]. More recently, for a cavity weakly modulated in the transverse and the longitudinal direction, one-dimensional so-called Bloch cavity solitons (BCSs) were identified [14,15]. The periodicity of the weak modulation has to be relatively large compared to the wavelength. This is detrimental to the advantage of a diffraction-managed soliton, allowing, for instance, for the reduction of the soliton width. In order to exploit the diffraction management at most, also the modulation should be on the smallest possible spatial scale. This leads to the idea of spatial solitons in an intracavity PhC with a strong index modulation on the wavelength scale.

Up to now CSs were treated as envelope solitons of either paraxial roundtrip models for forward and backward propagating waves, together with appropriate cavity boundary conditions, or a mean-field approach for the transmitted field derived from this. In this Rapid Communication we aim at a direct simulation of Maxwell's equations without an approximation. This was performed by means of a nonlinear version of the finite-difference time-domain (FDTD) method [18], allowing also for the treatment of structures with a strong dielectric modulation and for a direct proof of the above idea of diffraction-managed solitons. We identify different types of Bloch cavity solitons as a direct solution of Maxwell's equations. They are supported by a focusing or defocusing nonlinearity and may have an extremely small width. We then introduce a mean-field model based on Bloch waves to see how this compares to the direct approach.

Maxwell's equations with a Kerr nonlinearity in the time domain are

$$\nabla \times \mathbf{H}(\mathbf{r},t) = \frac{\partial \mathbf{D}(\mathbf{r},t)}{\partial t}, \quad \nabla \times \mathbf{E}(\mathbf{r},t) = -\mu_0 \frac{\partial \mathbf{H}(\mathbf{r},t)}{\partial t},$$
$$\mathbf{D}(\mathbf{r},t) = \varepsilon_0 \varepsilon(\mathbf{r}) \mathbf{E}(\mathbf{r},t) + \varepsilon_0 \chi^{(3)}(\mathbf{r}) |\mathbf{E}(\mathbf{r},t)|^2 \mathbf{E}(\mathbf{r},t), \quad (1)$$

where $\mathbf{E}$ and $\mathbf{H}$ are the real electric and magnetic fields, ε_0 and μ_0 are the permittivity and permeability constants, ε is the relative permittivity, and $\chi^{(3)}$ is the nonlinear coefficient. Note that within the FDTD method the divergence equations are automatically fulfilled for all times. Both the linear and nonlinear response are assumed to be instantaneous, i.e., material dispersion effects are neglected.

The configuration to start with is displayed in Fig. 1(a) (for details of the geometry parameters, see the caption). This can be considered as an effective index distribution of a membrane with finite thickness, for instance, in air. We restrict ourselves here to a 2D system in order to keep the computation time within a reasonable amount. Apart from possible out-of-plane losses which reduce the quality factor of the cavity, the results

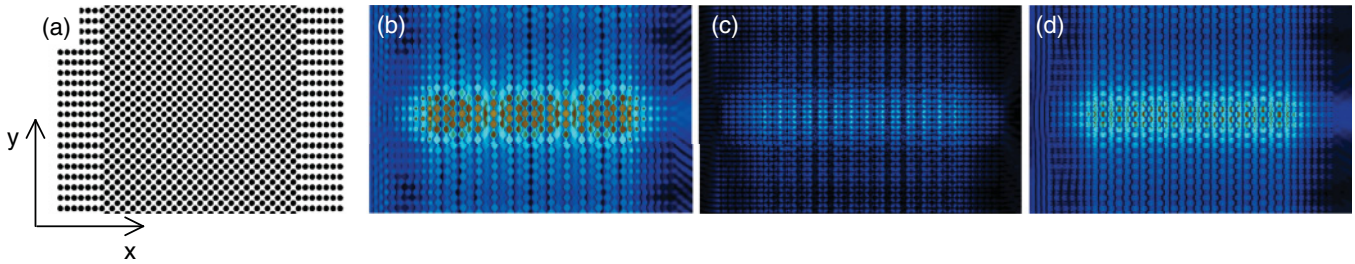

FIG. 1. (Color online) (a) Geometry of the all-PhC resonator (air holes in $\varepsilon = 12.25$). The radius of the holes is 0.12 μm. The period of the cavity PhC $a = 0.3$ μm (rotated by 45°), of the mirror PhCs $0.67\sqrt{2}a$ in the x direction and $\sqrt{2}a$ in the y direction. (b) H_z, (c) E_x, and (d) E_y components of the field of a BCS (case R2) for $\Delta = -3$ and $\sqrt{\chi^{(3)}}H_{z,\mathrm{in}} = 0.000\,15$ A/V. Displayed is the absolute value of the fundamental component of the time Fourier series of the field components. The computing window comprises 99 periods $\sqrt{2}a$ in the y direction of which 20 are shown. There are perfectly matched layers in the x direction and periodic boundary conditions in the y direction.

should also hold for a membrane. We consider here the TE case, i.e., the nonvanishing field components in the (x, y) plane are E_x, E_y, and H_z. In our geometry also the mirrors are made of photonic crystals. This allows for integrated fabrication and easy tuning of parameters, such as the cavity length and mirror reflectivity and thus the resonance frequencies and quality factor.

The linear and nonlinear properties of the resonator for plane wave incident fields are described in Refs. [19] and [20], respectively. In the latter the occurrence of bistability as a prerequisite for the existence of BCSs is discussed. To have bistability the cavity must be sufficiently detuned from a resonance frequency (see also below).

Pumping the cavity homogeneously, sufficiently detuned from a resonance frequency, and adding a spatio-temporal Gaussian to the pump cavity solitons can be excited. In our numerical experiments a line source in the y direction is added to H_z. Usually the homogeneous pump is within a range included in the region of bistability. Since CSs typically have a finite homogeneous plane wave or, in our case, a Bloch wave background, this one has to be stable for them to exist. An example with all field components is displayed in Fig. 1 (note that only a fraction of the computing window is shown). Due to the diffraction properties of the PhC, the nature of the cavity resonances can be different (see Fig. 2). In all cases we found BCSs. Adding a sufficiently phase-shifted spatio-temporal Gaussian to the homogeneous pump, the BCS can be erased again.

From Fig. 2 three different resonances can be identified (in terms of the mean-field coefficients $D^{(2)}$,$D^{(4)}$—see below). First of all, the lowest-frequency resonance at $\lambda_{\mathrm{res}} = 1.558\,67$ μm (resonance wavelengths are given for normal incidence $k_\perp = 0$) with a leading second-order term of the dispersion relation [normalized frequency $\Omega_{\mathrm{res}} = \omega_{\mathrm{res}}a/2\pi c = a/\lambda_{\mathrm{res}}$ as a function of $k_\perp$, where $D^{(n)} = \partial^n \Omega_{\mathrm{res}}(k_\perp)/\partial k_\perp^n$] corresponds to the usual cavity solitons (normal diffraction or positive $D^{(2)}$, focusing nonlinearity). Because the width and pump power of these BCSs are relatively large, we focus on the two other cases, denoted by R1 and R2. In the second case, R2, at $\lambda_{\mathrm{res}} = 1.509\,71$ μm, the next, fourth-order, term ($D^{(4)}$) of the dispersion relation has to be included since this term prevails over the second-order term ($D^{(2)}$) for $|k_\perp/G_\perp| > 0.1$. For $|k_\perp/G_\perp| < 0.1$ the diffraction is normal and hence the nonlinearity has to be focusing to have BCSs. Figure 1 displays an example of case R2. For this case the range of existence of BCSs, together with the bistable curve of steady extended Bloch states, is shown in Fig. 3. BCSs exist in and near the domain of bistability. The lower branch of the bistable curve is stable, and the upper branch is modulationally unstable.

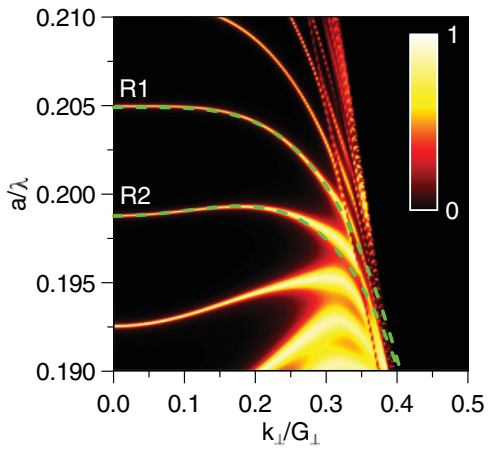

FIG. 2. (Color online) Transmittance of the linear resonator as shown in Fig. 1(a) as a function of the perpendicular wave vector (in terms of the perpendicular lattice vector $G_\perp = \sqrt{2}\pi/a$) and the frequency. For the value of a, see Fig. 1. The dashed lines are fourth-order polynomial fits.

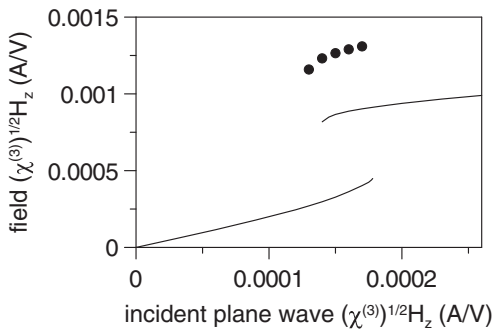

FIG. 3. Bifurcation diagram of case R2 for $\Delta = -3$. Solid lines denote Bloch waves, and dots denote BCSs. The diagram is recorded at a particular point of the system (maximum field strength).

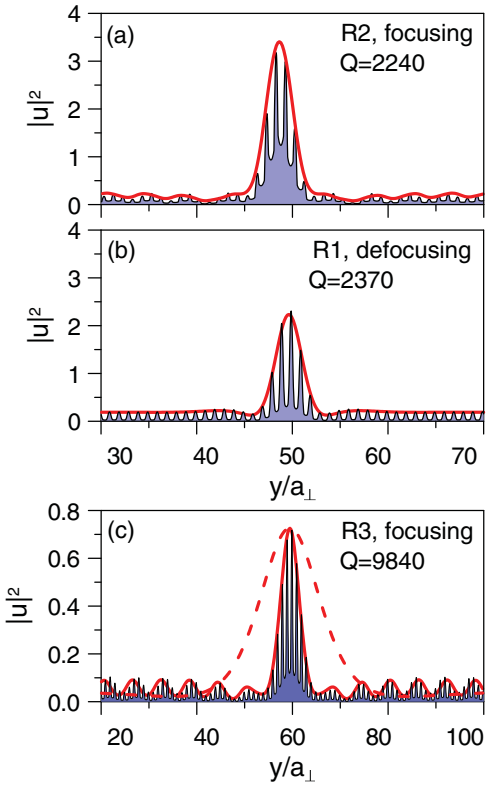

FIG. 4. (Color online) Comparison of BCSs from the direct approach (black filled line, slice in y direction within the cavity) and the mean-field model (red/gray line). Scaling refers to the latter one ($a_\perp = \sqrt{2}a$). (a) Case R2 for $\Delta = -3$, (b) case R1 for $\Delta = 3$, and (c) case R3 for $\Delta = -3$. The dashed line in (c) is a solution of the homogeneous cavity.

In the direct approach only stable states are accessible, although modulationally unstable ones are accessible since one transverse unit cell was used. The fourth-order term leads to radiating tails similar to Cherenkov radiation [cf. Fig. 4(a), black line] caused by resonant linear coupling (see Ref. [15]).

In the first case, R1, at $\lambda_{\text{res}} = 1.464\,16\ \mu$m, the leading term of the dispersion relation is fourth-order (vanishing $D^{(2)}$) with the same sign as in case R2 (negative fourth-order diffraction). To have cavity solitons the nonlinearity has to be defocusing here [cf. Fig. 4(b), black line]. In case R1 self-guiding of the cavity PhC is optimal (cf. also Ref. [20] for oblique incidence). Quality factors are $Q = 2240$ in case R2 and $Q = 2370$ in case R1. The quality factors can be adjusted easily by adding and removing rows of holes to and from the PhC mirrors. The minimum time to excite a BCS (decay of transient oscillations) is ∼10 ps (R1) or 20 ps (R2). The switching time increases with the external pump. Unlike in the mean-field model below, the switching time can be read off directly from the simulation.

Now the direct approach solving Maxwell's equations is compared to the mean-field model based on Bloch modes. Deriving equations for the slowly varying amplitudes of forward and backward propagating Bloch modes (cf. Ref. [21]) and applying the boundary conditions imposed by the mirrors as described in Ref. [22], the scaled mean-field equation for the transmitted amplitude u around one of the resonances (ω_{res}) is

$$i\frac{\partial u}{\partial t} + \frac{D^{(2)}}{2}\frac{\partial^2 u}{\partial y^2} - \frac{D^{(4)}}{24}\frac{\partial^4 u}{\partial y^4} + \gamma(i+\Delta)u + |u|^2 u = u_{\text{in}}, \tag{2}$$

where u_{in} is the external pump, γ is the loss, Δ is the detuning, and $D^{(2)}, D^{(4)}$ are the coefficients of the leading second- and fourth-order terms of the dispersion relation mentioned above (cf. also dashed lines in Fig. 2). Deriving Eq. (2) the loss is given by $1/\gamma = \tau_{\text{ph}} = 2Ln_{\text{g}}(\omega_{\text{res}})\rho/c(1-\rho^2)$, where τ_{ph} is the photon lifetime in the cavity, L is the cavity length, $n_{\text{g}}(\omega)$ is the group index of the cavity PhC, and ρ is the reflectivity of the mirrors (in terms of the field amplitudes). The quality factor of the cavity is then $Q = \omega_{\text{res}}\tau_{\text{ph}}/2$. For a given frequency ω the normalized detuning from a resonance ω_{res} is defined as $\Delta = \tau_{\text{ph}}(\omega - \omega_{\text{res}})$. Note that mean-field equations with up to fourth-order diffraction terms were used in Refs. [23] and [24] to obtain localized solutions. In Figs. 4(a) and 4(b) the resulting profiles are compared to the direct approach for the examples of cases R2 and R1 (red solid line). There is excellent agreement between the direct approach and the mean-field model, thus confirming that the latter can be used also for PhCs with a large modulation, provided that it is based on Bloch modes.

An important issue, e.g., for possible applications, are the pump power and the width of BCSs. Both should be as small as possible. To have a small external pump intensity I_{p}, the quality factor has to be large ($I_{\text{p}} \sim 1/Q^2$). But, on the other hand, for the purpose of fast all-optical switching, the photon lifetime and thus the quality factor should be small. Assuming, for instance, a maximum acceptable photon lifetime $\tau_{\text{ph}} = 15$ ps (switching frequency of order 0.1 THz) corresponds to a quality factor of approximately $Q = 10\,000$. As the photon lifetime, the width of cavity solitons also increases with Q. But here the cavity filled with a nonlinear PhC has an advantage. For a homogenous cavity the scaling of the width is as $\sqrt{Q}$. In the defocusing case R1 it scales only as $\sqrt[4]{Q}$, which is due to self-guiding. Usually a defocusing nonlinearity, for instance, operating a semiconductor near resonance (slightly

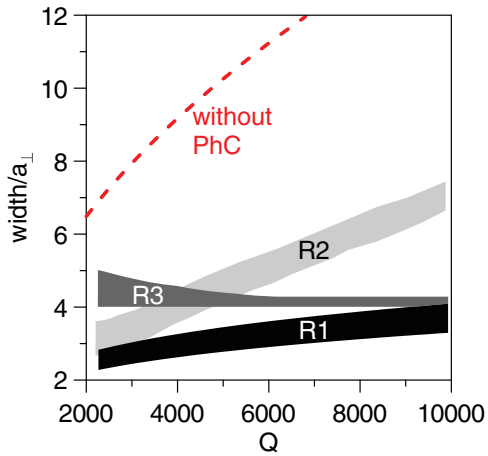

FIG. 5. (Color online) Minimal and maximal width of BCSs for the different cases versus the quality factor.

below the band gap), is associated with large absorption and slow relaxation times.

Toward a more optimal design of the present all-PhC cavity, we proceed as follows. First, adding two rows of holes to the PhC mirrors of the resonator increases the quality factor of the cavity to $Q = 9840$. Second, the cavity length L is increased by adding one row of holes. This shifts the resonance frequency and hence changes the sign of the diffraction with a small leading second-order term retaining the self-guiding mechanism. We refer to this design with a resonance wavelength $\lambda_{\mathrm{res}} = 1.479\,12\ \mu$m as case R3. In Fig. 4(c) a BCS solution of the direct approach is compared to the mean-field model, and the homogeneous cavity. At least, relative to the latter, the width is approximately four times smaller for case R3. This width corresponds to the free-space wavelength.

Since there is excellent agreement between the direct approach and the mean-field model, we use the latter for a more detailed analysis of the BCS width. First, from Fig. 5 we see that the optimal self-guided case R1 is much more advantageous than case R2. It can be seen that, as compared to the homogeneous cavity case (dashed line), the soliton is significantly narrower. In the optimal case R3 the width is almost independent on Q. Here the ratio between fourth- and second-order diffraction terms determines the absolute minimum of the BCS width [15].

In the direct approach it is easy to determine the pump power. For the optimal case R3 of Fig. 4(c), for example, the amplitude of the incident plane wave is approximately $H_{z,\mathrm{in}} = 3.8 \times 10^{-5}/\sqrt{|\chi^{(3)}|}$ A/V. From this the time-averaged longitudinal Poynting vector (pump intensity) is $I_{\mathrm{p}} = \langle S_x \rangle = \sqrt{\mu_0/(\varepsilon_0\varepsilon)}H_{z,\mathrm{in}}^2/2$. For the compound semiconductor GaAs with $\chi^{(3)} = 1.4 \times 10^{-18}\ \mathrm{m^2\,V^{-2}}$ this gives $I_{\mathrm{p}} = 5.5\ \mathrm{MW\ cm^{-2}}$. For an experimental realization in an air-suspended membrane of a thickness of $0.3\ \mu$m for a sufficiently broad Gaussian (10 solitons width) pump beam, a power of several 100 mW is required. The amplitude of the switching pulse is of the same order as the plane-wave pump. But due to the high Q, the switching time in case R3 is four times higher than in case R2.

In conclusion, we identified branches of Bloch cavity solitons in an all-photonic crystal resonator for different types of resonances by solving Maxwell's equations directly. We confirmed the validity of a mean-field model based on Bloch modes even for large modulation of the PhC, comparing it to the direct approach. The width and pump power of the BCSs were optimized by adjusting the quality factor and length of the cavity.

This work was supported by the German Federal Ministry of Education and Research (project PhoNa, Grant No. 03IS2101A), the Ministerio de Educación y Ciencia (Spain), and the Fondo Europeo de Desarrollo Regional (FIS2008-06024-C03-02).

[1] N. N. Rosanov and G. V. Khodova, J. Opt. Soc. Am. B **7**, 1057 (1990).
[2] A. J. Scroggie, W. J. Firth, G. S. McDonald, M. Tlidi, R. Lefever, and L. A. Lugiato, Chaos Solitons Fractals **4**, 1323 (1994).
[3] W. J. Firth and A. J. Scroggie, Phys. Rev. Lett. **76**, 1623 (1996).
[4] C. Etrich, U. Peschel, and F. Lederer, Phys. Rev. Lett. **79**, 2454 (1997).
[5] W. J. Firth and A. Lord, J. Mod. Opt. **43**, 1071 (1996).
[6] M. Tlidi, P. Mandel, and R. Lefever, Phys. Rev. Lett. **73**, 640 (1994).
[7] C. Etrich, D. Michaelis, U. Peschel, and F. Lederer, Chaos Solitons Fractals **10**, 839 (1999).
[8] C. Etrich, D. Michaelis, and F. Lederer, J. Opt. Soc. Am. B **19**, 792 (2002).
[9] D. Michaelis, U. Peschel, and F. Lederer, Phys. Rev. A **56**, R3366 (1997).
[10] M. Brambilla, L. A. Lugiato, F. Prati, L. Spinelli, and W. J. Firth, Phys. Rev. Lett. **79**, 2042 (1997).
[11] V. B. Taranenko, I. Ganne, R. J. Kuszelewicz, and C. O. Weiss, Phys. Rev. A **61**, 063818 (2000).
[12] V. B. Taranenko, I. Ganne, R. Kuszelewicz, and C. O. Weiss, Appl. Phys. B **72**, 377 (2001).
[13] V. B. Taranenko, K. Staliunas, and C. O. Weiss, Phys. Rev. Lett. **81**, 2236 (1998).
[14] K. Staliunas, O. Egorov, Y. S. Kivshar, and F. Lederer, Phys. Rev. Lett. **101**, 153903 (2008).
[15] O. A. Egorov, F. Lederer, and K. Staliunas, Phys. Rev. A **82**, 043830 (2010).
[16] D. Gomila and G.-L. Oppo, Phys. Rev. A **76**, 043823 (2007).
[17] O. A. Egorov and F. Lederer, Phys. Rev. A **76**, 053816 (2007).
[18] A. Taflove and S. C. Hagness, *Computational Electrodynamics: The Finite-Difference Time-Domain Method* (Artech House, Boston, MA, 2000).
[19] R. Iliew, C. Etrich, T. Pertsch, F. Lederer, and K. Staliunas, Opt. Lett. **33**, 2695 (2008).
[20] R. Iliew, C. Etrich, F. Lederer, and K. Staliunas, Opt. Lett. **35**, 3907 (2010).
[21] R. Iliew, C. Etrich, T. Pertsch, and F. Lederer, Phys. Rev. B **77**, 115124 (2008).
[22] D. Michaelis, U. Peschel, C. Etrich, and F. Lederer, IEEE J. Quantum Electron. **39**, 255 (2003).
[23] O. Egorov, F. Lederer, and K. Staliunas, Opt. Lett. **32**, 2106 (2007).
[24] L. Gelens, G. Van der Sande, P. Tassin, M. Tlidi, P. Kockaert, D. Gomila, I. Veretennicoff, and J. Danckaert, Phys. Rev. A **75**, 063812 (2007).